BANCO CENTRAL DE RESERVA DEL PERÚ

Exchange Rate Volatility in LATAM: Common and Idiosyncratic Factors*

Fernando J. Pérez Forero*

* Banco Central de Reserva del Perú

DT. N°. 2022-001
Serie de Documentos de Trabajo
Working Paper series
Mayo 2022

Exchange Rate Volatility in LATAM: Common and Idiosyncratic Factors*

Fernando J. Pérez Forero†

May 5, 2022

Abstract

This paper examines the volatility of the daily returns of the main Latin American currencies against the dollar (Brazil, Chile, Colombia, Mexico and Peru) over the last twenty years. Based on a simple Bayesian Stochastic Volatility framework, it is possible to identify the global synchronization factor of these currencies and distinguish it from the idiosyncratic component of each country. The global factor captured is highly correlated with popular volatility indicators, such as the VIX or the EPU of the US. We also find that the proportion of volatility explained by the global factor is significantly higher than that of the idiosyncratic component. Likewise, idiosyncratic volatility is much lower in the case of Peru compared to its peers in the region, with Brazil being the country with the most volatile component. Naturally, the characteristics of each market, credibility and confidence in the national currency, plus political uncertainty, and the exchange rate intervention of the central bank, play an important role in determining such volatilities.

Resumen

En este trabajo se analiza la volatilidad de los rendimientos diarios de las principales monedas latinoamericanas frente al dólar (Brasil, Chile, Colombia, México y Perú) durante los últimos veinte años. En base a un marco simple de volatilidad estocástica bayesiana, es posible identificar el factor de sincronización global de estas monedas y distinguirlo del componente idiosincrásico de cada país. El factor global capturado está altamente correlacionado con indicadores de volatilidad populares, como el VIX o el EPU de los EEUU. También encontramos que la proporción de volatilidad explicada por el factor global es significativamente mayor que la del componente idiosincrático. Asimismo, la volatilidad idiosincrática es mucho menor en el caso de Perú en comparación con sus pares de la región, siendo Brasil el país con el componente más volátil. Naturalmente, las características de cada mercado, la credibilidad y confianza en la moneda nacional, más la incertidumbre política y la intervención cambiaria del banco central, juegan un papel importante en la determinación de dichas volatilidades.

JEL Classification: C11, C32, F31

Key words: FX Markets, Stochastic Volatility

*I would like to thank participants at the BCRP's XXXIX Encuentro de Economistas, and seminar participants at the BCRP Research Seminar for their helpful comments and suggestions. The views expressed are those of the author and do not necessarily reflect those of the Central Reserve Bank of Peru. All remaining errors are mine.

†Deputy Manager of Monetary Policy Design, Central Reserve Bank of Peru (BCRP), Jr. Santa Rosa 441, Lima 1, Perú; Email address: fernando.perez@bcrp.gob.pe

1 Introduction

Foreign Exchange markets are crucial in determining the price of the local currency, i.e. the exchange rate against the US dollar or any other hard currency. In addition, the exchange rate is a extremely relevant relative price for macroeconomic equilibrium, especially in the case of small and open economies and emerging markets (Gadanecz and Mehrotra, 2013). Likewise, the volatility of the exchange rate is also a highly relevant variable for determining financial stability, which in many cases triggers Foreign Exchange Intervention (Bank for International Settlements, 2013), in particular when there is partial financial dollarization (Castillo and Medina, 2021), and also with different links in the productive chains and with dollar invoicing beyond their own foreign trade activity (Gopinath *et al.*, 2020).

In Latin American countries where the Inflation Targeting scheme is implemented, although they have a certain margin for independent fluctuations in the exchange rate based on macroeconomic fundamentals, we observe a partial co-movement in the daily returns of these currencies (see e.g. Gamboa-Estrada and Romero (2021)). This not an unknown phenomenon in Emerging Markets. For instance, Chiappini and Lahet (2020) examines these co-movements across different emerging markets in Asia using a dynamic latent factor model. Part of the explanation for this synchronization is the strong influence of the dollar in these economies, both in international trade and in financial markets (e.g., forward contracts or hedging operations, etc.). Thus, volatility clusters can be seen in certain common episodes, such as the 2008 International Financial Crisis, the 2013 Taper Tantrum, and the latest episode associated with the Covid-19 pandemic (see e.g. Fratzscher (2009) and Coudert *et al.* (2011)). Likewise, in each country a certain level of volatility can also be observed in episodes of greater uncertainty at the domestic level (generally due to political factors), such as those associated with presidential elections. In this context, although the vast majority portion of the literature focus the attention of finding the main determinants of exchange rates given these co-movements and to study their long run properties, our particular interest is to capture the common component of exchange rate volatility for the currencies of the region, and determine the fraction of total volatility explained by this factor. This will give us a clear idea of how much of the volatility of the exchange rate

is due to global or domestic factors.

Regarding the empirical literature about financial markets co-movement and volatility, we first find the work related with Synchronization of Currencies during Financial Crises (see e.g. Fratzscher (2009), who examines the period of the financial crisis of 2008, where a negative shock to the US economy strengthened the US dollar against different currencies, and Coudert *et al.* (2011) who study the Spillovers from advanced financial markets to currencies in emerging countries in terms of volatility using a regime-switching approach). There exists also empirical work related with Co-jumps in volatility, see e.g. Bollerslev *et al.* (2008) and Clements and Lia (2013); and Stochastic volatility and common drifting, see e.g. Qu and Perron (2013), Laurini and Mauad (2015), Carriero *et al.* (2016), Lee *et al.* (2017). Moreover, regarding Stochastic volatility and linear State Space Simulation, we can find the work of Jacquier *et al.* (1994) and Kim *et al.* (1998)[1], which are based on Bayesian Simulation of Linear State-Space Systems using the Kalman Filter and Smoother as in Carter and Kohn (1994) and Durbin and Koopman (2002). Other applications using FX Volatility data from Latin American Countries can be found in Rodríguez (2017), Alanya and Rodríguez (2018), Alanya and Rodríguez (2019) who follow Omori *et al.* (2007), Rodríguez *et al.* (2019), among others.

Our main findings point out that Exchange Rate returns volatility in LATAM is highly synchronized, although there are domestic factors that also play a role. Moreover, the estimated global factor is highly correlated with other global measures of uncertainty, such as the VIX[2] and the Economic Policy Uncertainty (EPU) of the United States. Our estimated common factor explains a higher portion of total volatility for each country under study with respect to idiosyncratic volatility. This result is especially relevant during the Great Financial Crisis of 2008, the Taper Tantrum of 2013, and the recent Covid-19 Pandemic episode. Nevertheless, there exists some room for idiosyncratic factors to be relevant for FX volatility, and we find that, in most of the cases, a higher idiosyncratic volatility can be related with pre-electoral periods.

[1] See also the correction suggested by Del Negro and Primiceri (2015).

[2] The VIX is a real-time volatility index created by the Chicago Board Options Exchange (CBOE).

The document is organized as follows: section 2 describes the model, section 3 describes the estimation procedure, section 4 discusses the main results, and section 5 concludes.

2 The model

Consider the following Stochastic Volatility model for the Exchange Rate daily returns $r_{i,t}$. Define $r_{i,t} = 100 * (e_{i,t} - e_{i,t-1})/e_{i,t-1}$ as the returns[3] for each country $i = 1, \ldots, N$, with the following dynamic representation:

$$r_{i,t} = \alpha_i + exp\left(\frac{b_i h_t}{2} + \frac{h_{i,t}}{2}\right) v_{i,t}, \qquad v_{i,t} \sim i.i.d.N\left(0, 1\right) \tag{1}$$

The common volatility factor h_t has an *a priori* law of motion that is given by:

$$h_t = h_{t-1} + \eta_t, \qquad \eta_t \sim i.i.d.N\left(0, \sigma_\eta^2\right) \tag{2}$$

and the corresponding law of motion for the idiosyncratic volatility component $h_{i,t}$ is given by:

$$h_{i,t} = h_{i,t-1} + \epsilon_{i,t}, \qquad \epsilon_{i,t} \sim i.i.d.N\left(0, \sigma_{\epsilon_i}^2\right) \tag{3}$$

In both cases we assume a random walk, since this is a more parsimonious representation relative to an $AR(1)$ (see e.g. Primiceri (2005)), and therefore we avoid the cost of estimating additional parameters[4]. Moreover, the element $b_i > 0$ is a loading parameter that captures the relative contribution of the common factor h_t to the whole log-volatility, i.e. the term $\left(\frac{b_i h_t}{2} + \frac{h_{i,t}}{2}\right)$ at each period t, and α_i is an intercept coefficient that captures the average long term return of the exchange rate.

[3] Although it is often common in the literature to use instead $r_{i,t} = 100 * (ln\left(e_{i,t}\right) - ln\left(e_{i,t-1}\right))$, this is a linear approximation of the growth rate that might deliver different results for large daily variations, such as in the crisis episodes, and thus could lead us to underestimate the actual volatility. In addition, different sources of financial information, e.g. websites from Reuters, etc., usually report the daily percentage change, and this is what markets observe in order to make decisions. As a result, the piece of information relevant in this context is the % change.

[4] In many papers related with stochastic volatility it is assumed an AR(1) law of motion. However, this comes at the cost of imposing strong priors for stationarity, since the autorregressive parameter usually delivers a posterior mode very close to 1, and with an intercept that is far from being statistically different from 0. See e.g. Kim *et al.* (1998).

The specified model is conditionally linear and Gaussian, and thus we can exploit standard Bayesian Markov Chain Monte Carlo (MCMC) techniques to simulate the posterior distribution of the objects of interest. Given the specified structure, the state-space system is highly tractable for our purpose. A crucial point for the identification of the common factor h_t and the idiosyncratic ones $h_{i,t}$ is the assumption of independence across innovations in the transition equations (2) and (3). Given the mentioned structure, we are then able to disentangle the common component from the idiosyncratic ones in a simultaneous estimation procedure, i.e. we estimate the model for the entire set of observables $i = 1, \ldots, N$ in a unified way. The specified model is similar to other approaches that use Stochastic volatility and common drifting, see e.g. Qu and Perron (2013), Laurini and Mauad (2015), Carriero *et al.* (2016), Lee *et al.* (2017).

3 Bayesian Estimation

3.1 State Space Model specification

The model (1)-(2)-(3) can be re-written as a state-space system with time varying matrices[5], so that:

$$y_t = D_t \alpha_t + \varepsilon_t, \qquad \varepsilon_t \sim N(0, H_t) \tag{4}$$

$$\alpha_t = A_t \alpha_{t-1} + R_t \eta_t, \qquad \eta_t \sim N(0, Q_t) \tag{5}$$

Posterior simulation of vector α_t is performed following Carter and Kohn (1994) and Durbin and Koopman (2002) algorithms. Because of the presence of Stochastic Volatility, the measurement equation is linearly approximated following Kim *et al.* (1998) and, in order to ensure the convergence of the algorithm, we use the correction proposed by Del Negro and Primiceri (2015). More specifically, taking squares and then logs in the measurement equation (1), and considering an offset constant of $\underline{c} = 0.001$ to avoid numerical issues such as taking the log of zero, we get:

$$ln\left(r_{i,t} - \alpha_i + \underline{c}\right)^2 = b_i h_t + h_{i,t} + u_{i,t} \tag{6}$$

[5] see e.g. Harvey (1989) and Kim and Nelson (1999), among others.

Since $u_{i,t} = ln\left(v_{i,t}^2\right) \sim log\chi^2$, this element is approximated using a mixture of 7 normals:

$$f\left(u_{i,t}\right) \approx \sum_{j=1}^{7} q_j f_N\left(u_{i,t} \mid m_j - 1.2704, v_j^2\right) \tag{7}$$

Denote $\psi = \left(\Theta, \alpha^T\right)$ as the parameter set of the model, then the complete posterior distribution is:

$$p\left(\psi \mid y^T\right) = p\left(\Theta, \alpha^T \mid y^T\right) \propto p\left(\Theta\right) p\left(\alpha_0\right) \prod_{t=1}^{T} p\left(y_t \mid \alpha_t, \Theta\right) p\left(\alpha_t \mid \alpha_{t-1}, \Theta\right) \tag{8}$$

where $\alpha_t = \left[h_t, \{h_{i,t}\}_{i=1}^N\right]'$ and $y_t = \left[\{r_{i,t}\}_{i=1}^N\right]'$, and where Θ contains the remaining structural parameters of the model.

3.2 Data and estimation setup

For the empirical implementation, we use Exchange Rate daily returns for Brazil, Chile, Colombia, Mexico and Peru, which is depicted in Figure 1. The sample of analysis covers the dates between January 1, 2002 and October 31, 2021[6] and the source is Central Bank Websites as well as Reuters. In this context, volatility clusters can be seen in certain common episodes, such as the Great Financial Crisis (GFC) of 2008, the 2013 *Taper Tantrum*, and the latest episode associated with the Covid-19 pandemic. In the same figure, in each country a certain level of volatility can also be observed in episodes of greater uncertainty at the domestic level (generally due to political factors), such as those associated with presidential elections. The data seems to be stationary in mean, so that we will consider a constant intercept α_i for each country. Moreover, the support of the distribution of returns seems to be time varying for each country under study, so that in this case a structure that considers a time varying volatility is also appropriate. Then, with simple inspection of data and news of the day is impossible to determine whether a change in volatility can be attributed to domestic or global factors, although we can elicit some hypothesis based on experts judgment.

[6]For the interested reader, Daily Exchange Rate Data in levels is depicted in Figure B.11.

Figure 1: **Exchange Rate Daily Returns - LATAM (2002-2021)**
Units expressed in %

(a) Brazil (b) Chile (c) Colombia

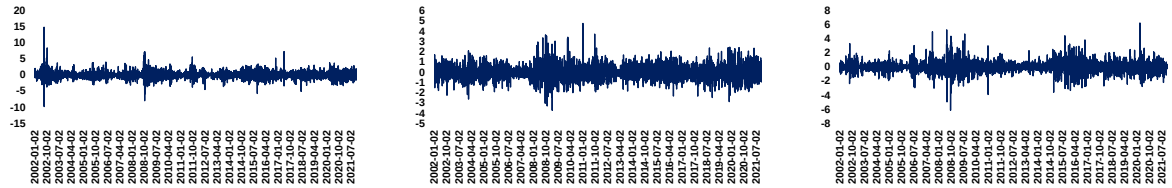

(d) Mexico (e) Peru

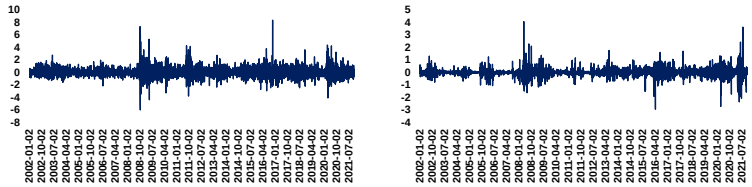

3.3 Prior specification

We set the prior distribution for different parameter blocks in Table 1. In first place, since we have assumed that the *a priori* law of motion of the factors h_t and $h_{i,t}$ follows a random walk, this is the case of a diffuse filter, i.e. we cannot solve for a steady state distribution in equations (2) and (3), and therefore we set the initial point for the Kalman Filter as $h_0 = h_{i,0} = 0$ with a large variance, so that we set $V_h = 10$. Then, the prior distribution for the variance parameters σ_η^2 and $\sigma_{\epsilon_i}^2$ is a conjugated Inverse-Gamma with a mean of $\underline{\sigma}^2 = 0.1$ and with degrees of freedom $d_0 = 10$ (see.e.g. Carriero *et al.* (2016)). The prior for the intercept parameter α_i is a conjugated normal distribution, with zero mean and a large variance $V_\alpha = 10$, meaning that this is also a diffuse prior. Finally, the prior for the loading coefficient b_i is normal centered in 0.5 and setting a standard deviation to ensure that it takes only positive values[7].

[7]We can alternatively use a Beta distribution instead, but we do not want to discard the possibility of $b_i > 1$.

Parameter	Distribution	Hyper-parameters
$h_{i,0}$	Normal	$N\left(0, V_h\right)$
h_0	Normal	$N\left(0, V_h\right)$
σ_η^2	Inverse-Gamma	$IG\left(d_0 \times \underline{\sigma}^2, d_0\right)$
$\sigma_{\epsilon_i}^2$	Inverse-Gamma	$IG\left(d_0 \times \underline{\sigma}^2, d_0\right)$
α_i	Normal	$N\left(\underline{\alpha}, \underline{V}_\alpha\right)$
b_i	Normal	$N\left(\underline{b}, \underline{V}_b\right)$

Table 1: Prior Distribution for the parameter set

3.4 Gibbs Sampling

The simulation algorithm for the posterior distribution of the parameter set ψ in (8) is as follows. We set $k = 1$ and consider K as the total number of draws and r^T as the full data set, then given the initial conditions for each block ψ_0 simulate:

1. Simulate s_i^T from $p\left(s_i \mid r_i^T, \psi_{-s_i}\right)$ for each $i = 1, \ldots, N$: Discrete Distribution
2. Simulate $\left\{h_i^T\right\}$ from $p\left(h_i^T \mid r_i^T, \psi_{-h_i^T}\right)$ for each $i = 1, \ldots, N$: SS-Volatility
3. Simulate $\left\{h^T\right\}$ from $p\left(h^T \mid r^T, \psi_{-h^T}\right)$: SS-Volatility
4. Simulate σ_η^2 from $p\left(\sigma_\eta^2 \mid r^T, \psi_{-\sigma_\eta^2}\right)$: Inverse-Gamma
5. Simulate $\sigma_{\epsilon_i}^2$ from $p\left(\sigma_{\epsilon_i}^2 \mid r_i^T, \psi_{-\sigma_{\epsilon_i}^2}\right)$ for each $i = 1, \ldots, N$: Inverse-Gamma
6. Simulate α_i from $p\left(\alpha_i \mid r_i^T, \psi_{-\alpha_i}\right)$ for each $i = 1, \ldots, N$: Conditional Linear Regression
7. Simulate b_i from $p\left(b_i \mid r_i^T, \psi_{-b_i}\right)$ for each $i = 1, \ldots, N$: Metropolis-Hastings step
8. If $k < K$, set $k = k + 1$ and back to step 1.

See details for each block in Appendix A. We run the Gibbs sampler for $K = 500,000$ and discard the first $250,000$ draws in order to minimize the effect of initial values. In order to reduce the serial correlation across draws, we set a thinning factor of 100. As a result, we have

5,000 draws for conducting inference. The acceptance rate of the metropolis-step associated with b_i is around 30% for each $i = 1, \ldots, N$. After simulation and convergence, we are ready to present the results of the empirical exercise in the next section.

4 Results

4.1 Main Results

Given the proposed simulation algorithm, and using daily returns data for Brazil, Chile, Colombia, Mexico and Peru for the episode January 2002 to October 2021, the volatility of the exchange rate is obtained for each of the countries under analysis. The estimated volatility can take negative values because it is on a logarithmic scale. Estimated volatilities are depicted in Figure 2. Important peaks can be seen, as in the case of 2008 and 2020, a phenomena that will be explained below. Likewise, in Peru, the increase in volatility during the last episode of political uncertainty stands out, reaching levels similar to those of the Great Financial Crisis of 2008.

Figure 2: **Estimated FX Volatility**

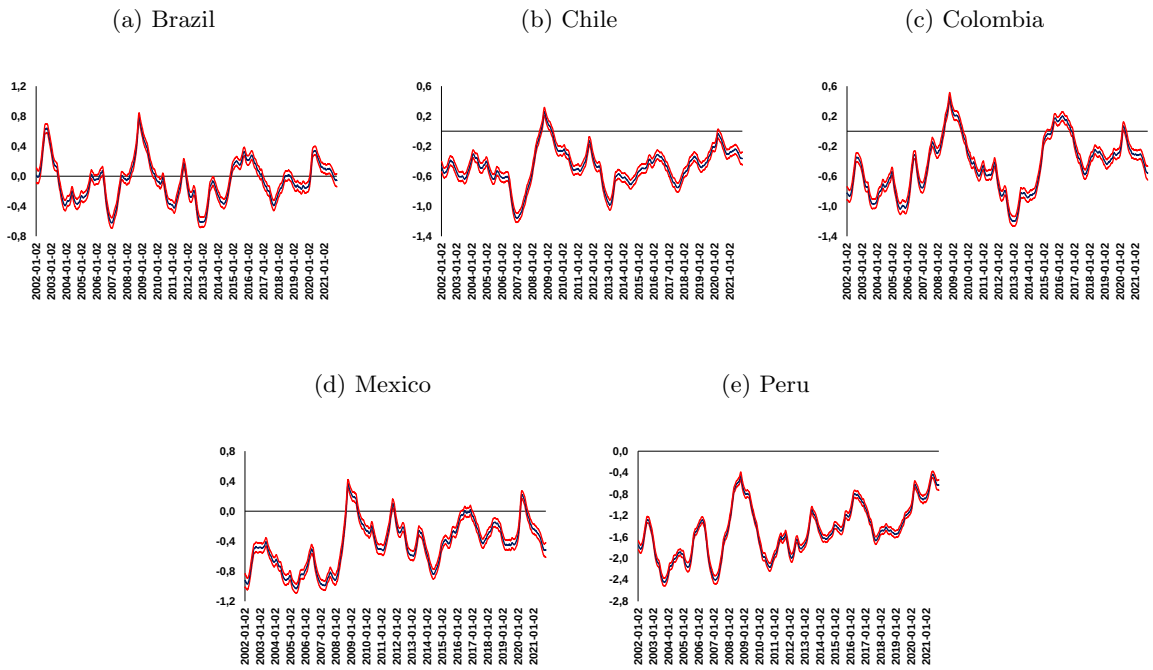

Given the specified model, these volatilities can be decomposed into a common factor and an idiosyncratic one. The common factor is depicted in Figure $_h$. In each of the shaded global episodes a significant and persistent increase in this factor can be seen, which translates into greater synchronization in the returns of the region's currencies. In general, this is channeled through news or signals received by the market, and this results in the determination of a new equilibrium market price based on the supply and demand, both on the side of spot operations and derivative instruments. It is worth highlighting the fact that this factor reached its historical peak during the 2008 Financial Crisis, not being surpassed by subsequent events, although the Covid-19 pandemic event almost reached it. It is also worth noting that the estimated global factor is highly correlated with other global measures of uncertainty, such as the VIX or the US EPU, as it is shown in Figure 4.

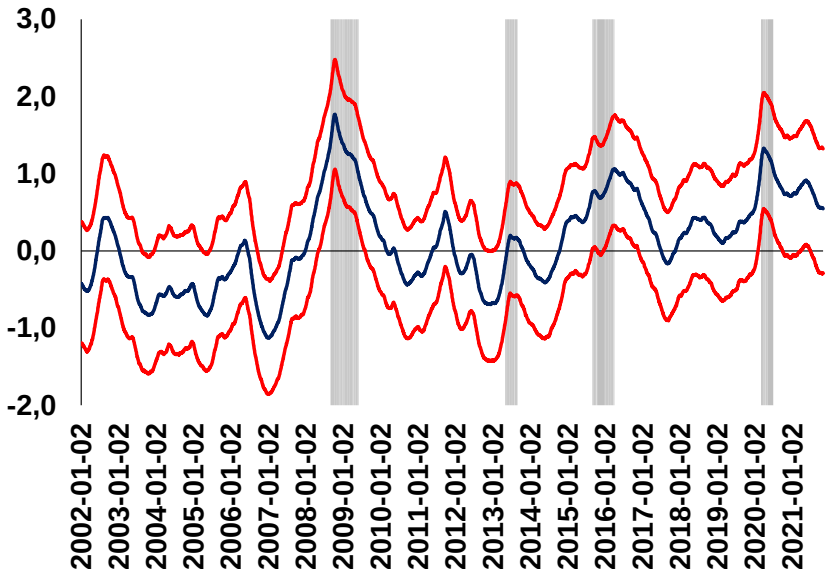

Figure 3: Log-Common Factor Volatility (h_t)

Figure 4: **Log-Common Factor Volatility and Volatility Indexes**

(a) VIX

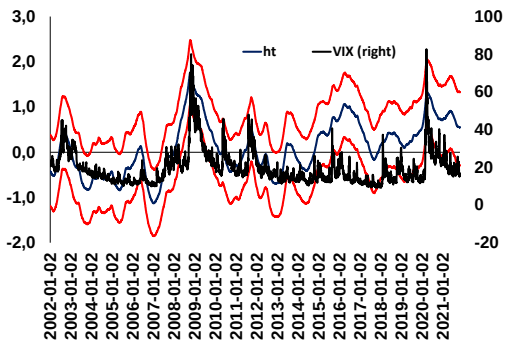

(b) EPU-US

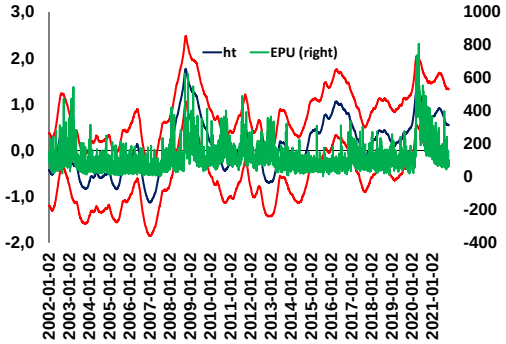

Although it has been shown that exchange rate volatility in the region is highly synchronized, it is important to note that there are domestic factors that also influence it. Thus, for each of the countries under analysis, the idiosyncratic volatility component is depicted in Figure 5, also on a logarithmic scale. Consequently, in most cases an increase in idiosyncratic volatility related to these electoral periods is observed, which is quite noticeable, especially in the Peruvian case, followed by the case of Brazil, Mexico, Colombia and Chile. Another important point that can be seen from this result is that jumps in idiosyncratic volatility are also observed in some cases after global events. Although the effect associated with the synchronization factor has been isolated, the latter is due to a contagion effect derived from global uncertainty, which is amplified by the deterioration of domestic conditions. A clear example of this are the aforementioned global crises, as well as the recent pandemic episode. On the other hand, it is worth highlighting the lower magnitude of idiosyncratic volatility in the Peruvian case with respect to its peers in the region, which would be associated with the greater credibility of the Peruvian Sol (PEN) acquired in recent years, and also the fact that participating agents internalize that the Central Bank could intervene in the market to mitigate this volatility.

Figure 5: **Log-Idiosyncratic Volatility**

(a) Brazil

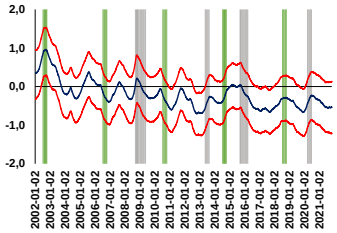

(b) Chile

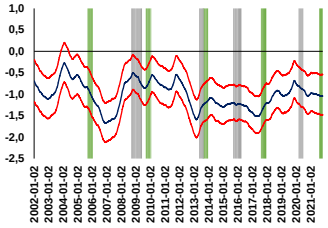

(c) Colombia

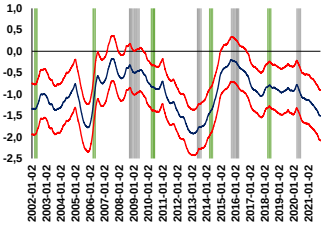

(d) Mexico

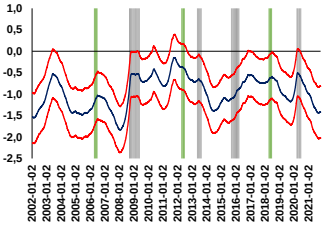

(e) Peru

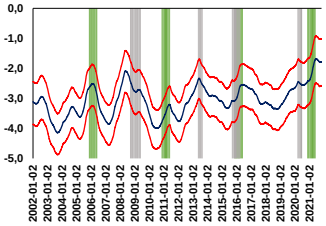

4.2 An Indicator of Relative Contribution

Finally, in order to quantify which factor is the one that predominates in the aggregate volatility, an indicator is constructed for each $i = 1, \ldots, N$ from the results of the estimation of the model.

$$I_{i,t} = \frac{exp\left(\frac{b_i * h_t}{2}\right)}{exp\left(\frac{h_{i,t}}{2}\right)} \tag{9}$$

It is important to note that in the construction of this indicator the coefficient ($b_i > 0$) plays a crucial role, since it represents the direct impact that global volatility has on that of each country, and said estimated coefficients range between 0.5 and 1.0 for these economies under analysis. Moreover, given the constructed indicator, it is possible to test the hypothesis $H_0 : I_{i,t} > 1$ for each country, which would mean that the contribution of the global factor is significantly higher than the local one.

Figure 6 shows the resulting indicator for each country, and the green line $I_{i,t} = 1$ is drawn

to carry out the hypothesis contrast. These results show that, with the exception of Brazil, followed by Mexico, in most cases and for almost the entire sample it is observed that the global factor is the predominant factor in exchange rate volatility. For reference, the gray areas associated with the global events mentioned above have also been added here. It can thus be clearly seen that this relative contribution intensifies during these marked events, making it clear that this effect is not constant over time. Likewise, in terms of magnitude, the case of Peru stands out, where this indicator is substantially higher than in other countries (although it has been decreasing in recent months), which is also the result of the lower idiosyncratic volatility mentioned above.

Figure 6: **Relative Contribution Indicator**

(a) Brazil

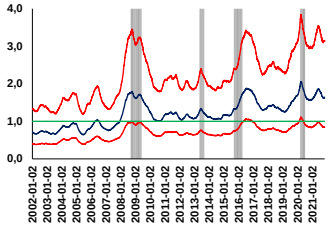

(b) Chile

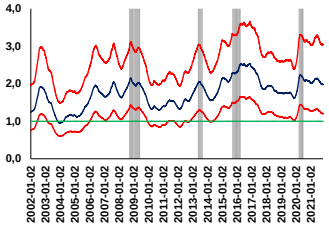

(c) Colombia

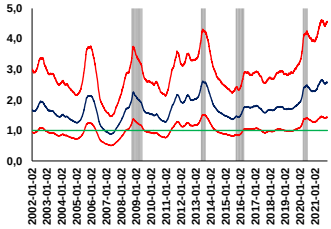

(d) Mexico

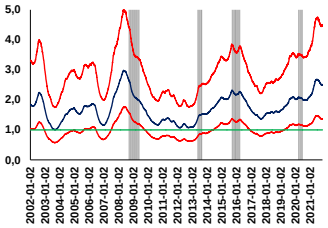

(e) Peru

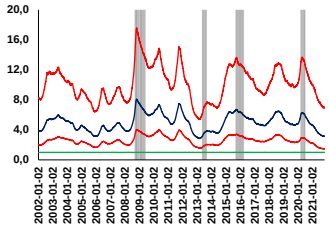

5 Concluding Remarks

The exchange rate volatility of Brazil, Chile, Colombia, Mexico and Peru has been estimated using bayesian methods, and both the common and idiosyncratic component have been identified. The estimated common factor shows a high correlation with global events, such as different

crisis episodes, and this is consistent with other popular uncertainty measures in the market (VIX and EPU of the US). Likewise, the contribution of the global factor is generally relatively greater than the domestic one, with the exception of the case of Brazil, where the greater contribution in the case of Peru stands out. Finally, idiosyncratic or domestic volatility is usually highly correlated with pre-electoral periods.

Part of our research agenda is to dig more on the differences both in the weight of the global factor and in idiosyncratic volatility. A first idea is related to the specific characteristics of each market, capital flows, as well as to the exchange intervention carried out by each central bank. Another interesting theme is to compare our estimated idiosyncratic volatility with local political uncertainty indexes for each country under study. Finally, our estimated common volatility factor could also be compared with other global measures, such as the estimated volatility of the DXY. The interested reader could also apply this methodology to other financial assets or variables, such as commodity prices, stock market indexes, etc.

A Gibbs Sampling details

1. **Block 1**: Simulate s_i^T from $p\left(s_i^T \mid r_i^T, \psi_{-s_i}\right)$ for each $i = 1, \ldots, N$: Discrete Distribution (Kim *et al.*, 1998) Conditional on the values of the other parameters, the terms $v_{i,t}^2$ in equation (1) are observable, so that we can sample the states, i.e. the elements of s^T independently from the following a discrete distribution:

$$p\left(s_{i,t} = j \mid v_{i,t}^2, h_{i,t}, h_t\right) \propto f_N\left(ln\left(v_{i,t}^2 + 0.001\right) \mid b_i h_t + h_{i,t} + m_j - 1.2704, v_j^2\right) \tag{A.1}$$

where $j \in \{1, \ldots, 7\}$ is the index for the state of the mixture of normals, $f_N\left(x \mid \mu, \sigma^2\right)$ is referred to the normal density function with mean μ, variance σ^2 and evaluated at point x. The values for means, variances and weights for the mixture of normals can be found in the following table.

s	$P(s = j)$	m_j	v_j^2
1	0.00730	−10.12999	5.79596
2	0.10556	−3.97281	2.61369
3	0.00002	−8.56686	5.17950
4	0.04395	2.77786	0.16735
5	0.34001	0.61942	0.64009
6	0.24566	1.79518	0.34023
7	0.25750	−1.08819	1.26261

Table A.2: $log\chi^2$ Distribution Approximation (Kim *et al.*, 1998)

2. **Block 2**: Simulate $\{h_{i,t}\}_{t=1}^T$ from $p\left(h_{i,t} \mid r_i^T, \psi_{-h_{i,t}}\right)$ for each $i = 1, \ldots, N$: SS-Volatility

In order to sample volatilities $h_{i,t}$ we proceed for each $i = 1, \ldots, N$ as follows: Given the parameter values of the model and the measurement equation (1), compute the innovations $\tilde{\zeta}_{i,t} = ln\left(r_{i,t} - \alpha_i + \underline{c}\right)^2 - b_i h_t$ and specify the following measurement equation

$$\tilde{\zeta}_{i,t} = h_{i,t} + u_{i,t} \tag{A.2}$$

where $u_{i,t} \sim log\left(\chi^2\right)$ is approximated through a mixture of 7 normal distributions:

$$f\left(u_{i,t}\right) \approx \sum_{j=1}^{7} q_j f_N\left(u_{i,t} \mid m_j - 1.2704, \upsilon_j^2\right) \tag{A.3}$$

In addition, we have the transition equation (3)

$$h_{i,t} = h_{i,t-1} + \epsilon_{i,t}, \qquad \epsilon_{i,t} \sim i.i.d.N\left(0, \sigma_{\epsilon_i}^2\right)$$

As a result, equations $(A.2) - (3)$ form a state-space system, so that we can simulate h_i^T following Kim *et al.* (1998), i.e. using the algorithm of Carter and Kohn (1994) conditional on the discrete variable s_i^T and given the prior in Table 1.

3. **Block 3**: Simulate $\{h_t\}_{t=1}^T$ from $p\left(h_t \mid r^T, \psi_{-h_t}\right)$: SS-Volatility

In order to sample volatilities h_t we proceed as follows: Given the parameter values of the model and the measurement equation (1), compute the innovations $\tilde{v}_{i,t} = ln\left(r_{i,t} - \alpha_i + \underline{c}\right)^2 - h_{i,t}$ and specify the following measurement equation

$$\begin{bmatrix} \tilde{v}_{1,t} \\ \tilde{v}_{2,t} \\ \cdots \\ \tilde{v}_{N,t} \end{bmatrix} = \begin{bmatrix} b_1 \\ b_2 \\ \cdots \\ b_N \end{bmatrix} h_t + \begin{bmatrix} u_{1,t} \\ u_{2,t} \\ \cdots \\ u_{N,t} \end{bmatrix} \tag{A.4}$$

where each $u_{i,t} \sim log\left(\chi^2\right)$ is approximated through a mixture of 7 normal distributions:

$$f\left(u_{i,t}\right) \approx \sum_{j=1}^{7} q_j f_N\left(u_{i,t} \mid m_j - 1.2704, \upsilon_j^2\right) \tag{A.5}$$

In addition, we have the transition equation (2)

$$h_t = h_{t-1} + \eta_t, \qquad \eta_t \sim i.i.d.N\left(0, \sigma_\eta^2\right)$$

As a result, equations $(A.4) - (2)$ form a state-space system, so that we can simulate h^T

following Kim *et al.* (1998), i.e. using the algorithm of Carter and Kohn (1994) conditional on the discrete variables s^T and given the prior in Table 1.

4. **Block 4**: Simulate σ_η^2 from $p\left(\sigma_\eta^2 \mid r^T, \psi_{-\sigma_\eta^2}\right)$: Inverse-Gamma Distribution

   Recall the transition equation (2)

$$h_t = h_{t-1} + \eta_t, \qquad \eta_t \sim i.i.d.N\left(0, \sigma_\eta^2\right)$$

   Variance parameter σ_η^2 is simulated using an Inverse-Gamma distribution. Given the prior $\sigma_\eta^2 \sim IG\left(d_0 \times \underline{\sigma}^2, d_0\right)$ and the remaining model parameters $\psi_{-\sigma_\eta^2}$, the posterior distribution is:

$$p\left(\sigma_\eta^2 \mid r^T, \psi_{-\sigma_\eta^2}\right) = IG\left(d_0 \times \underline{\sigma}^2 + \sum_{t=2}^{T} u_t^2, d_0 + T - 1\right) \tag{A.6}$$

   where $u_t = h_t - h_{t-1}$.

5. **Block 5**: Simulate $\sigma_{\epsilon_i}^2$ from $p\left(\sigma_{\epsilon_i}^2 \mid r_i^T, \psi_{-\sigma_{\epsilon_i}^2}\right)$ for each $i = 1, \ldots, N$: Inverse-Gamma Distribution

   Recall the transition equation (3)

$$h_{i,t} = h_{i,t-1} + \epsilon_{i,t}, \qquad \epsilon_{i,t} \sim i.i.d.N\left(0, \sigma_{\epsilon_i}^2\right)$$

   Variance parameters $\sigma_{\epsilon_i}^2$ are simulated using an Inverse-Gamma distribution. Given the prior $\sigma_{\epsilon_i}^2 \sim IG\left(d_0 \times \underline{\sigma}^2, d_0\right)$ and the remaining model parameters $\psi_{-\sigma_{\epsilon_i}^2}$, the posterior distribution for each $i = 1, \ldots, N$ is:

$$p\left(\sigma_{\epsilon_i}^2 \mid r_i^T, \psi_{-\sigma_{\epsilon_i}^2}\right) = IG\left(d_0 \times \underline{\sigma}^2 + \sum_{t=2}^{T} u_{i,t}^2, d_0 + T - 1\right) \tag{A.7}$$

   where $u_{i,t} = h_{i,t} - h_{i,t-1}$.

6. **Block 6**: Simulate α_i from $p\left(\alpha_i \mid r_i^T, \psi_{-\alpha_i}\right)$ for each $i = 1, \ldots, N$: Conditional Linear

Regression

Recall the measurement equation (1).

$$r_{i,t} = \alpha_i + exp\left(\frac{b_i h_t}{2} + \frac{h_{i,t}}{2}\right) v_{i,t}$$

Given the prior in Table 1, i.e. $\alpha_i \sim \mathrm{N}(\underline{\alpha}, \underline{V}_\alpha)$. then the posterior distribution of α_i is Normal:

$$p\left(\alpha_i \mid r_i^T, \psi_{-\alpha_i}\right) = N\left(\overline{\alpha}_i, \overline{V}_i\right) \tag{A.8}$$

with

$$\overline{V}_i = \left(\underline{V}^{-1} + \sum_{t=1}^{T} \frac{1}{H_{i,t}}\right)^{-1} \tag{A.9}$$

$$\overline{\alpha}_i = \overline{V}\left(\underline{V}^{-1}\underline{\alpha} + \sum_{t=1}^{T} \frac{r_{i,t}}{H_{i,t}}\right) \tag{A.10}$$

and where $H_{i,t} = exp\left(b_i h_t + h_{i,t}\right)$.

7. **Block 7**: Simulate b_i from $p\left(b_i \mid r_i^T, \psi_{-b_i}\right)$ for each $i = 1, \ldots, N$: Metropolis-Hastings step

Recall the measurement equation (1).

$$r_{i,t} = \alpha_i + exp\left(\frac{b_i h_t}{2} + \frac{h_{i,t}}{2}\right) v_{i,t}$$

Because $v_{i,t} \sim i.i.d.N\left(0,1\right)$, then we can evaluate the log-likelihood function for the parameter b_i. For this purpose, we have to take into account that for each $t = 1, \ldots, T$ we have the density:

$$p\left(r_{i,t} \mid b_i, \psi_{-b_i}\right) = N\left(\alpha_i, exp\left(b_i h_t + h_{i,t}\right)\right) \tag{A.11}$$

so that

$$p\left(r_i^T \mid b_i, \psi_{-b_i}\right) = \prod_{t=1}^{T} p\left(r_{i,t} \mid b_i, \psi_{-b_i}\right) \tag{A.12}$$

Given the prior in Table 1, i.e. $p(b_i) = N(\underline{b}, \underline{V}_b)$, then the posterior distribution of b_i is

$$p\left(b_i \mid r_i^T, \psi_{-b_i}\right) \propto p\left(r_i^T \mid b_i, \psi_{-b_i}\right) p(b_i) \tag{A.13}$$

In order to sample from this posterior distribution, we specify the proposal density to draw candidates b_i^*

$$b_i^* \sim N\left(b_i^{old}, c_b\right) \tag{A.14}$$

where b_i^{old} is the current draw of b_i and $c_b > 0$ is a constant fixed with the aim of getting an acceptance rate between 0.2 and 0.4. Then, the following kernel is evaluated

$$\alpha_{bi} = min\left[1, \frac{p\left(b_i^* \mid r_i^T, \psi_{-b_i^*}\right)}{p\left(b_i^{old} \mid r_i^T, \psi_{-b_i^{old}}\right)}\right] \tag{A.15}$$

so that b_i^* is accepted as a draw from $p\left(b_i \mid r_i^T, \psi_{-b_i}\right)$ with probability α_{bi}.

B Additional Figures

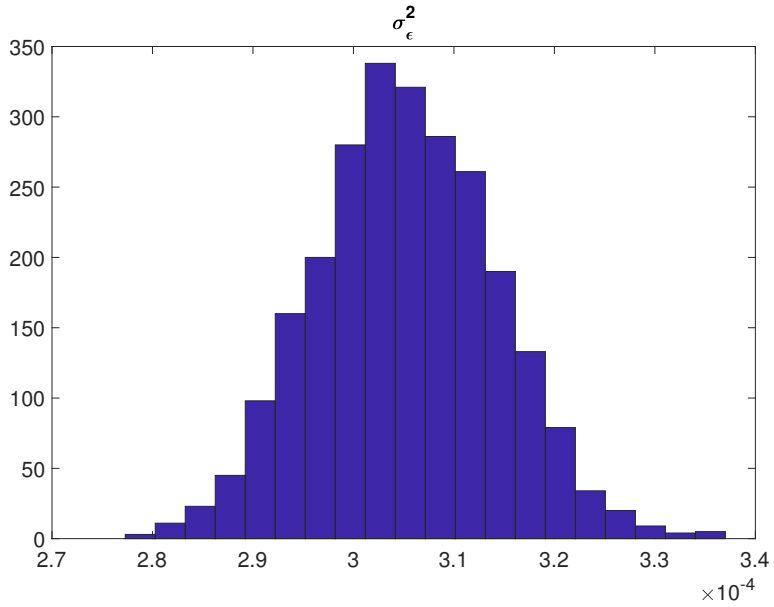

Figure B.7: Posterior Distribution of Variance parameters $\left(\sigma_\eta^2\right)$

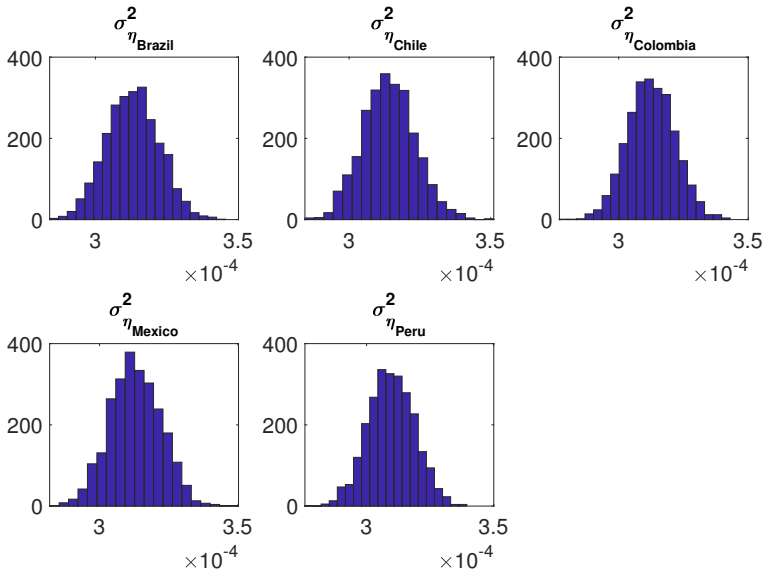

Figure B.8: Posterior Distribution of Variance parameters $\left(\sigma^2_\eta\right)$

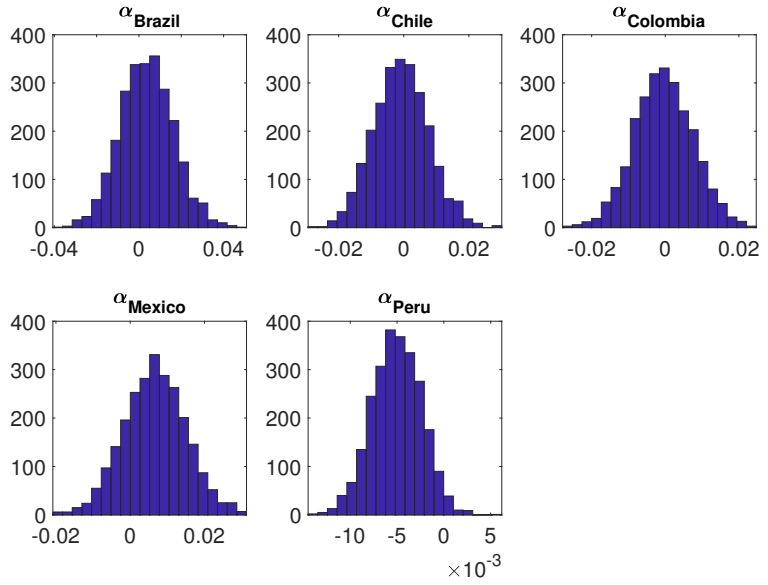

Figure B.9: Posterior Distribution of Intercept coefficients (α_i)

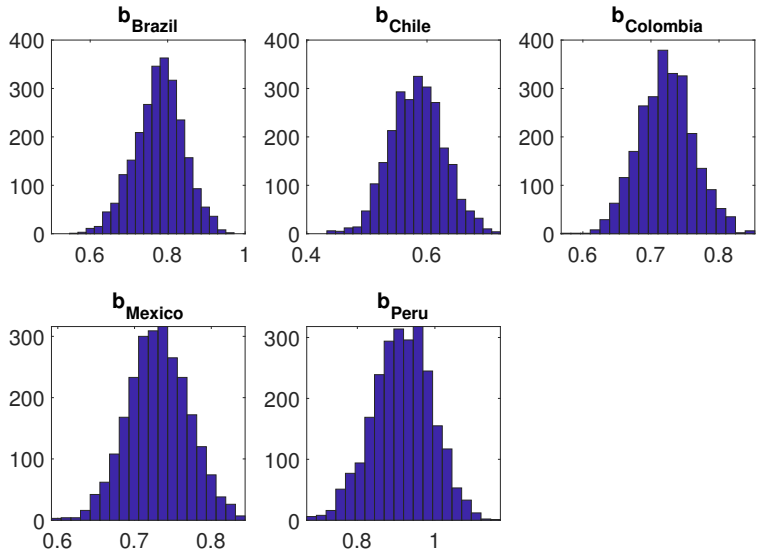

Figure B.10: Posterior Distribution of Loading parameters (b_i)

Figure B.11: **Exchange Rate Data - LATAM (2002-2021)**
Units expressed in National Currency per US$

(a) Brazil

(b) Chile

(c) Colombia

(d) Mexico

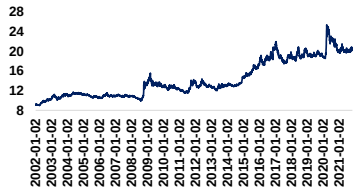

(e) Peru

References

Alanya, W. and Rodríguez, G. (2018). Stochastic volatility in the peruvian stock market and exchange rate returns: A bayesian approximation. *Journal of Emerging Market Finance*, **17** (3), 354–385.

— and Rodríguez, G. (2019). Asymmetries in volatility: An empirical study for the peruvian stock and forex markets. *Review of Pacific Basin Financial Markets and Policies*, **22** (1), 1–18.

Bank for International Settlements (2013). *Market volatility and foreign exchange intervention in EMEs: what has changed?* Bank for International Settlements.

Bollerslev, T., Law, T. H. and Tauchen, G. (2008). Risk, jumps, and diversification. *Journal of Econometrics*, **144** (1), 234–256.

Carriero, A., Clark, T. E. and Marcellino, M. (2016). Common drifting volatility in large bayesian vars. *Journal of Business and Economic Statistics*, **34** (3), 375–390.

Carter, C. K. and Kohn, R. (1994). On gibbs sampling for state space models. *Biometrika*, **81** (3), 541–553.

Castillo, P. and Medina, J. P. (2021). *Foreign Exchange Intervention, Capital Flows, and Liability Dollarization*. Working Papers 2021-006, Banco Central de Reserva del Perú.

Chiappini, R. and Lahet, D. (2020). Exchange rate movements in emerging economies - global vs regional factors in asia. *China Economic Review*, **60**, 101386.

Clements, A. and Lia, Y. (2013). The dynamics of co-jumps, volatility and correlation, nCER Working Paper Series 91.

Coudert, V., Couharde, C. and Mignon, V. (2011). Exchange rate volatility across financial crises. *Journal of Banking Finance*, **35** (11), 3010–3018.

Del Negro, M. and Primiceri, G. (2015). Time varying structural vector autoregressions and monetary policy: A corrigendum. *Review of Economic Studies*, **82**, 1342–1345.

Durbin, J. and Koopman, S. (2002). A simple and efficient simulation smoother for state space time series analysis. *Biometrika*, **89** (3), 603–615.

Fratzscher, M. (2009). What explains global exchange rate movements during the financial crisis? *Journal of International Money and Finance*, **28** (8), 1390–1407, the Global Financial Crisis: Causes, Threats and Opportunities.

Gadanecz, B. and Mehrotra, A. (2013). The exchange rate, real economy and financial markets. In B. f. I. Settlements (ed.), *Sovereign risk: a world without risk-free assets?*, vol. 73, Bank for International Settlements, pp. 11–23.

Gamboa-Estrada, F. and Romero, J. V. (2021). *Common and idiosyncratic movements in Latin-American Exchange Rates*. Borradores de Economia 1158, Banco de la Republica de Colombia.

Gopinath, G., Boz, E., Casas, C., Díez, F. J., Gourinchas, P.-O. and Plagborg-Møller, M. (2020). Dominant currency paradigm. *American Economic Review*, **110** (3), 677–719.

Harvey, A. C. (1989). *Forecasting, Structural Time Series Models and the Kalman Filter*. Cambridge University Press.

Jacquier, E., Polson, N. G. and Rossi, P. E. (1994). Bayesian analysis of stochastic volatility models. *Journal of Business and Economic Statistics*, **20** (1), 69–87.

Kim, C.-J. and Nelson, C. R. (1999). *State-Space Models with Regime-Switching: Classical and Gibbs-Sampling Approaches with Applications*. MIT Press.

Kim, S., Shephard, N. and Chib, S. (1998). Stochastic volatility: Likelihood inference and comparison with ARCH models. *The Review of Economic Studies*, **65** (3), 361–393.

Laurini, M. and Mauad, R. (2015). A common jump factor stochastic volatility model. *Finance Research Letters*, **12**, 2–10.

Lee, E., Han, D., Ito, S. and Nayga, R. (2017). A common factor of stochastic volatilities between oil and commodity prices. *Applied Economics, Taylor and Francis Journals*, **49** (22), 2203–2215.

Omori, Y., Chib, S., Shephard, N. and Nakajima, J. (2007). Stochastic volatility with leverage: Fast and efficient likelihood inference. *Journal of Econometrics*, **140** (2), 425–449.

Primiceri, G. (2005). Time varying structural vector autoregressions and monetary policy. *Review of Economic Studies*, **72**, 821–852.

Qu, Z. and Perron, P. (2013). A stochastic volatility model with random level shifts and its applications to sp 500 and nasdaq return indices. *The Econometrics Journal*, **16** (3), 309–339.

Rodríguez, G. (2017). Modeling latin-american stock and forex markets volatility: Empirical application of a model with random level shifts and genuine long memory. *The North American Journal of Economics and Finance*, **42**, 393–420.

Rodríguez, G., Cunya, J. A. O. and Tanaka, J. C. G. (2019). An empirical note about estimation and forecasting latin american forex returns volatility: the role of long memory and random level shifts components. *Portuguese Economic Journal*, **18** (2), 107–123.